Quantification of variability interactions in multilead ECG: applicability as function of variability and noise levels

Almeida, Rute
Rocha, Ana Paula
Universidade do Porto, Faculdade de Ciências and CMUP
R Campo Alegre 687
4169-007 Porto, Portugal
E-mail: rbalmeid@fc.up.pt, aprocha@fc.up.pt

Martínez, Juan Pablo
Laguna, Pablo
University of Zaragoza, Comm Techn Group, Aragon Institute of Eng Research CIBER-BBN
María de Luna, 1
50018 Zaragoza, Spain
E-mail: jpmart@unizar.es, laguna@unizar.es

Introduction

The electrocardiogram (ECG) is the surface record of the cardiac electrical activity. Abnormalities may conduct or predispose to life threatening conditions and hence the ECG is an indispensable diagnostic tool. The phenomena correspond to different ECG waves (P, Q, R, S, T) which can be used to access both durations and beat-to-beat variations (Fig. 1 - 2). The RR intervals series $x_{\mathrm{RR}}(n)$ (time between consecutive R waves) is the simplest of ECG extracted series and is currently used as heart rate series (HR); the QT intervals series $x_{\mathrm{RR}}(n)$ (time from the QRS complex onset to the T wave end) is usually considered as an index of cardiac repolarization. The evaluation of the cardiac rhythms is a problem of major importance. Abnormal QT lengths and beat-to-beat variability (QTV), have been associated to several pathological conditions and increased risk situations. The RR interval variability (HRV) strongly affects QTV, even so the quantification of this relation has not been established yet.

In a previous work [Almeida *et al.* (2004, 2006*b*)] the QTV vs HRV interactions were explored by a dynamic linear approach using AR and ARARX models with automatic orders selection. This strategy was validated with simulated data series and illustrated in real data. A single-lead based delineation system of ECG peaks and waves was applied over the ECG to assess the series variability.

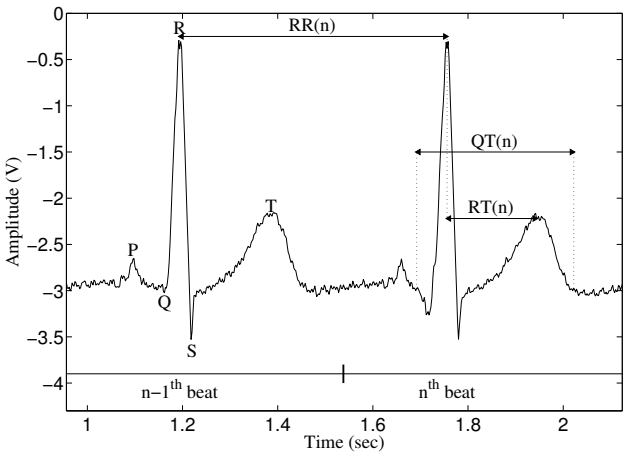

Figure 1: Some ECG waves and intervals.

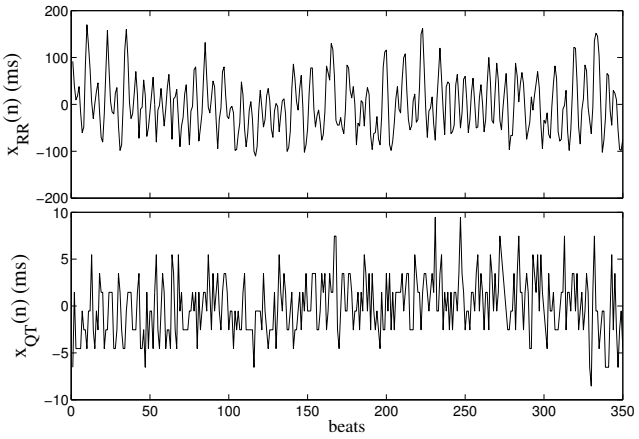

Figure 2: Example of real simultaneous RR and QT variability series corrected for the mean.

The clinical ECG recordings often contain several leads, that is simultaneous signals according to different cardiac axes given by different positions of electrodes on the torso. Multilead ECGs give different perspectives of the involved electrical phenomena and allow to have a spatial perception. Choosing a particular lead for delineation determines a "point of view", and thus different latencies on the waves's onsets and ends are found in the different leads. Combining adequately the information provided by multiple leads is essential for the correct location of the waves' boundaries.

In this work the methodology is validated over artificially simulated multilead ECG signals, with different QTV and noise contamination levels. Indicative limits of applicability as function of QTV and noise levels are determined and presented graphically in way to be well suited for use in practise.

Automatic ECG delineation

The RR and QT intervals limits are located using the automatic wavelet transform (WT) based delineation systems previously developed [Martínez *et al.* (2004); Almeida *et al.* (2006*a*)]. The prototype wavelet considered produces a WT description with a derivative like behaviour, well suited for locating peaks and slopes. Each feature is located in the scales according to its typical frequencies.

The QRS complex produces modulus maxima lines across the WT scales corresponding to higher frequencies; in each lead the single-lead (SL) based R peak is located as the zero crossing between the main WT extremes with reverse polarity associated to QRS complex [Martínez *et al.* (2004)]. The multilead (ML) based R peak location is taken as the median of the 3 SL based locations.

The QT boundaries are located using a ML strategy described in [Almeida *et al.* (2006*a*)], that has proven to outperform the SL system for QT measuring. The methodology considers the canonical representation of the electrical heart vector (EHV) obtained with 3 orthogonal ECG leads, also called vectocardiogram (VCG), which is often recorded and can be obtained by linear transformations from other lead systems. Very briefly, this system uses WT spatial loops (WT of the 3 leads) in a multistep iterative search of a *better* spatial lead for delineation improvement. Given the WT prototype used, the WT loop is proportional to the VCG derivative and describes the EHV evolution. Thus, the linear fitting line (in total least squares sense) to the WT loop gives the main EHV direction $\vec{U}$. The projection on the WT loop over $\vec{U}$ produces a constructed WT like signal, potentially presenting steeper slopes and more adequate for boundaries location using threshold based criteria.

Parametric modelling of QTV-HRV relations

The parametric methodology explores QTV - HRV interactions assuming an open loop linear $ARARX_q$ model (Fig. 3) [Porta *et al.* (1998)]. The QTV trend is assumed to result from two uncorrelated sources, one driven by RR and another resulting from an AR process with a white noise input $w_{\mathrm{QT}}(n)$. The series $x_{\mathrm{RR}}(n)$ is explained by an AR_p model. The white noises $w_{\mathrm{RR}}(n)$ and $w_{\mathrm{QT}}(n)$ are uncorrelated stationary zero mean, with variances λ^2_{RR} and λ^2_{QT}. Optimal values between 2 and 18 automatically selected: first the order p of the AR is chosen by AIC and q, for simplicity assumed for all ARARX model polynomials, is taken as the one minimizing the multivariate AIC for the given p. The power spectral function of $x_{\mathrm{QT}}(n)$, $S_{\mathrm{QT}}(F)$, can be computed as the sum of two partial spectra expressing the contributions related ($S_{\mathrm{QT|RR}}(F)$) and unrelated ($S_{\mathrm{RR|RR}}(F)$) to RR interval, that is

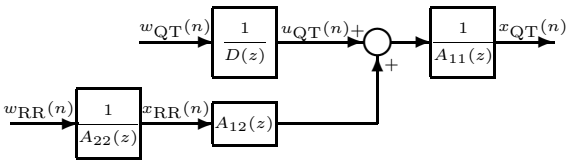

Figure 3: Model of QTV versus HRV interactions

$$(1) \qquad S_{\mathrm{QT|RR}}(F) = T_R \lambda^2_{\mathrm{RR}} \left| \frac{A_{12}(z)}{A_{11}(z)A_{22}(z)} \right|^2_{z=e^{j2\pi F T_R}}, \quad S_{\mathrm{QT|QT}}(F) = T_R \lambda^2_{\mathrm{QT}} \left| \frac{1}{A_{11}(z)D(z)} \right|^2_{z=e^{j2\pi F T_R}},$$

(T_R stands for mean RR). The power for each QTV fraction in any frequency band $\mathcal{B}$, $\left(P^{\mathcal{B}}_{\mathrm{QT|RR}}, P^{\mathcal{B}}_{\mathrm{QT|QT}}\right)$, can be calculated by decomposing these spectra and summing the contributions of the poles located in $\mathcal{B}$; $R^{\mathcal{B}}_{\mathrm{QT|RR}} = 100P^{\mathcal{B}}_{\mathrm{QT|RR}} / \left[P^{\mathcal{B}}_{\mathrm{QT|RR}} + P^{\mathcal{B}}_{\mathrm{QT|QT}}\right]$ gives the relative fraction of the QTV driven by RR. Typical frequency bands $\mathcal{B}$ in HRV studies were used: LF (0.04-0.15 Hz) and HF (0.15-0.4 Hz). In system identification, the residuals $w_{\mathrm{RR}}(n)$ and $w_{\mathrm{QT}}(n)$ were considered to be uncorrelated white noises if their normalized auto / cross correlations were not different from zero (5% significance bilateral tests, both for the first 40 lags and for all lags). Model orders not corresponding to white noise / uncorrelated residuals, or producing a negative global contribution in a frequency band were excluded.

Simulation set-up

The validation of the methodology described is done over signals with known QTV fractions (related and unrelated with HRV), generated assuming that the linear model in Fig. 3 holds.

To obtain reference parameters for the model first were constructed auxiliary series $\tilde{x}_{\mathrm{QT}}(n)$, $\tilde{x}_{\mathrm{QT}}(n) = a\left(\sqrt{x_{\mathrm{RR_{Re}}}(n)} + \sqrt{x_{\mathrm{RR_{Ti}}}(n)}\right) + b$, based in the classical Bazett's correction formula. It allows to obtain QTV series resulting from 2 uncorrelated sources in a nonlinear way. Independent $x_{\mathrm{RR}}(n)$ realizations agreeing to spectra typically found at supine rest (Re) and head-up tilt (Ti) situations were considered, with $T_R = 1$ sec. The parameter b allows to set a zero mean while a allows to adjust the standard deviation (σ_{QT}) of $\tilde{x}_{\mathrm{QT}}(n)$ (QTV level). In this work $\sigma_{\mathrm{QT}} = \{17, 13, 10, 8, 5 \text{ and } 3\}$ ms, covering the interval of values between extreme situations found in healthy subjects. Parametric model identification in equations considering $x_{\mathrm{RR}}(n) = x_{\mathrm{RR_{Re}}}(n)$ and $x_{\mathrm{QT}}(n) = \tilde{x}_{\mathrm{QT}}(n)$, provides the values for the reference coefficients values and the residual noise standard deviation (λ^r_{QT}) for the simulation. Parametric decomposition with this reference parameters allows to obtain a reference value for $R^{\mathcal{B}}_{\mathrm{QT|RR}}$.

Once the reference model parameters were obtained, 50 uncorrelated realizations were simulated. To also evaluate the methodology in a more realistic context were constructed artificial *3-lead* ECG signals at 500 Hz matching the previous simulated series. Real ECG signals, besides morphologic beat-to-beat variability, are also affected by extra cardiac factors, such as respiration or muscular activity. In order to consider these factors, a 3-lead realistic noise was extracted from a real ECG and added to the artificial signal, considering different signal-to-noise ratio values (SNR). Test datasets were defined as the variability series corresponding to 350 consecutive beats free of outliers (admissible segments) of each realizations, considering the series directly simulated from reference model parameters - *clean* (C) - or applying ML delineation over the artificial signals - data sets $S_{(SNR)}$, $SNR \in \{\infty, 30, 25, 20, 15, 10\}\, dB$, with $SNR = \infty$ for the case with no added noise.

Performance evaluation

The model identification over the series in each data set and the parametric decomposition allow to estimate the relative fraction of the QTV driven by RR in each frequency band $\mathcal{B}$ ($\hat{R}^{\mathcal{B}}_{\mathrm{QT|RR}}$). The errors ($\varepsilon^{\mathcal{B}}$) in this quantification were defined as difference between estimated and reference ratios.

The distribution of $\varepsilon^{\mathcal{B}}$ is presented in Fig. 4 (left side). Negative bias in $\varepsilon^{\mathcal{B}}$ indicates that $R^{\mathcal{B}}_{\mathrm{QT|RR}}$ was underestimated. For $SNR \leq 15dB$, delineation errors produced more outliers and less admissible segments are found. Even in qualified segments, the parametric method is hardly applicable. A performance reduction was expected for lower QTV levels. However, with $\sigma_{\mathrm{QT}} \in \{3, 5\}$ ms lower $\varepsilon^{\mathcal{B}}$ was obtain than with $\sigma_{\mathrm{QT}} \in \{8, 10\}$ ms, which can be related with the specific model parameters used in simulation, rather than with QTV. In particular, it was found less than 25% error:

- in over 74% of segments in data sets with SNR > 15 dB and $\sigma_{\mathrm{QT}} > 3$ ms in LF band;

- in over 95% of segments in data sets with SNR > 20 dB and $\sigma_{\mathrm{QT}} > 10$ ms in HF band.

These results can be used to establish an indicative range of applicability of the proposed methods, that is, the levels of QTV and SNR for which the QTV fractions can be estimated with an admissible error (here assumed as less than 25%). For a more intuitive use, the applicability as function of QTV and SNR can be summarized graphically, as presented in Fig. 4 (right). In these plots, for each SNR level it was addressed the minimum σ_{QT} for which an error tolerance degree of 25% was accomplished, that is the $\varepsilon^{\mathcal{B}}$ quartile box was within the horizontal ligther grey band in $\varepsilon^{\mathcal{B}}$ distribution in the rigth of Fig. 4. Values for σ_{QT} are presented only if data from at least one QT model fulfilled the criteria and the grey darker rectangles correspond to the transition between reference models.

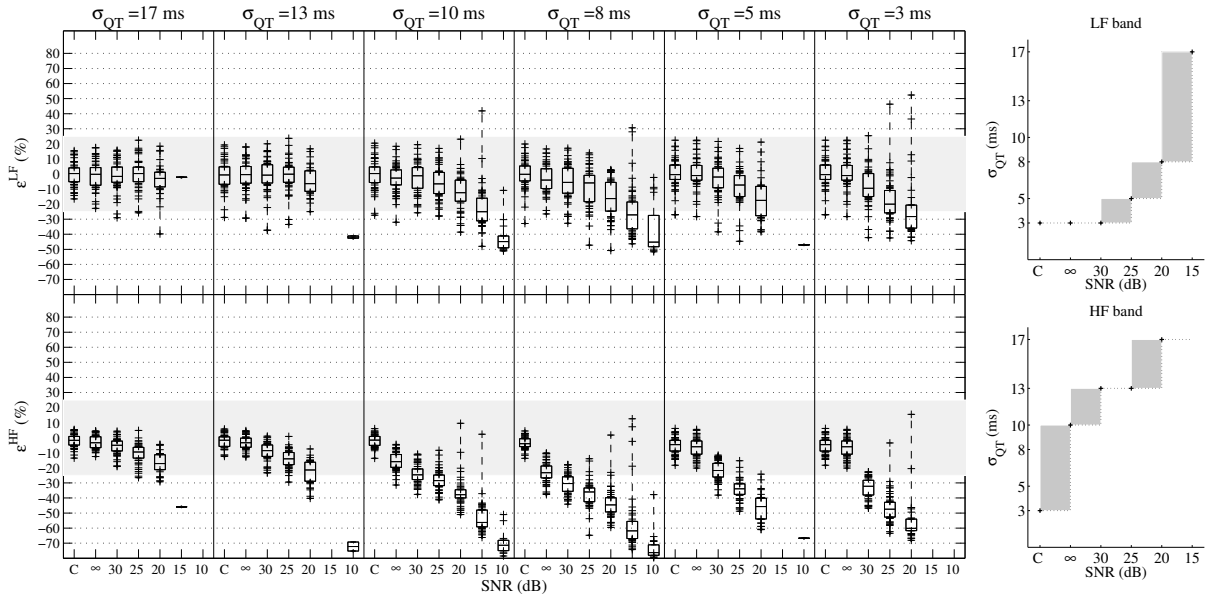

Figure 4: Distributions of $\varepsilon^{\mathcal{B}}$ and indicative limits of applicability (C stands for the *clean* series).

Conclusions

The results allow to conclude that for the LF band the methods were able to estimate satisfactory the QTV fractions in most of the files, for $SNR > 15dB$ and $\sigma_{QT} > 3$ ms; the HF band can only be consided with $SNR > 20dB$ and, even so, in a critical way.

REFERENCES

Almeida, R., A. P. Rocha, E. Pueyo, J. P. Martínez and P. Laguna (2004). Modelling short term variability interactions in ECG: QT versus RR. In: *Computational Statistics 2004*. Physica-Verlag. pp. 597–604.

Almeida, R., J. P. Martínez, A. P. Rocha, P. Laguna and S. Olmos (2006*a*). Automatic multilead VCG based approach for QT interval measurement. In: *Computers in Cardiology 2006*. Vol. 33. pp. 369–372.

Almeida, R., S. Gouveia, A. P. Rocha, E. Pueyo, J. P. Martínez and P. Laguna (2006*b*). QT variability and HRV interactions in ECG: Quantification and reliability. *IEEE Trans. Biomed. Eng.* **53**, 1317–1329.

Martínez, J. P., R. Almeida, S. Olmos, A. P. Rocha and P. Laguna (2004). Wavelet-based ECG delineator: evaluation on standard databases. *IEEE Trans. Biomed. Eng.* **51**, 570–581.

Porta, A., G. Baselli, E. Caiani, A. Malliani, F. Lombardi and S. Cerutti (1998). Quantifying electrocardiogram RT-RR variability interactions. *Med. Biol. Eng. Comput.* **36**, 27–34.